Adaptative and ancient co-evolution of integrons with *Xanthomonas* genomes

Elena Colombi[1,2 *], Timothy M. Ghaly[1,2], Vaheesan Rajabal[1,2], Liam D.H. Elbourne[1,2], Michael Gillings[1] & Sasha Tetu[1,2]

[1] School of Natural Sciences, Macquarie University, Sydney, NSW, 2109, Australia
[2] ARC Centre of Excellence in Synthetic Biology, Sydney, NSW, 2109, Australia
*Corresponding author: elena.colombi@mq.edu.au

Keywords: genome evolution, horizontal gene transfer, niche adaptation, plant-pathogen, mobile genetic elements

ABSTRACT

Integrons are genetic elements that facilitate gene acquisition. They have been extensively studied in clinical bacteria, but their evolutionary role in phytopathogens remains underexplored. Here, we analysed complete genomes of *Xanthomonas* species to investigate the origin, distribution, and functional dynamics of integrons in this genus. We found that 93% of genomes harboured integrons. The integron-integrase gene *intI* was predominantly located downstream of *ilvD*, indicating an ancestral acquisition of integrons, predating diversification within the genus. Phylogenetic analyses support vertical inheritance of *intI*, with the exception of rare horizontal gene transfer events, notably in *X. arboricola*. Despite their widespread presence, full-length *intI* genes and active integron platforms are only retained in some species, especially *X. campestris*, which shows high integron gene cassette variability and functional integron activity. In contrast, species such as *X. cissicola* and *X. phaseoli* exhibit widespread *inI* inactivation, likely occurring early in their divergence, leading to more stable cassette arrays and conserved integron-associated phenotypes. The number and diversity of genes within cassette arrays varied significantly by species and, to a lesser extent, by the ecological context of plant host cultivation. While most cassettes encoded proteins without a known function, those with annotated roles were associated with stress response mechanism, competitive exclusion, and plant-associated functions. Together, our findings demonstrate that integrons in *Xanthomonas* likely originated from a single ancient acquisition event, preceding genus-wide speciation, and have co-evolved with *Xanthomonas* pathovars as they adapted to distinct plant hosts.

IMPACT STATEMENT

This study provides the first comprehensive genus-wide analysis of integron evolution and dynamics in *Xanthomonas*, a globally distributed and versatile plant pathogen. Integrons are

genetic platforms that allow horizontal transfer of genes. They are well characterised in human pathogens where they mediate transfer of antibiotic resistance genes, but little is known about their role in plant associated bacteria. We showed that in *Xanthomonas* the integron platform was ancestrally acquired, yet integrons have undergone repeated lineage-specific inactivation events. Despite widespread erosion of integron activity, some species such as *X. campestris* maintain robust and functionally diverse integrons that continue to shape genome plasticity. Notably, high cassette diversity, combined with the presence of rare and often uncharacterized genes within these arrays (some potentially involved in environmental sensing or host interaction) suggest that integrons may serve as reservoirs of adaptive potential. Our findings reshape current views of integron function beyond antibiotic resistance and highlight their long-term role in microbial evolution, niche adaptation, and genome innovation in plant-associated bacteria.

DATA SUMMARY

The authors confirm all supporting data, code and protocols have been provided within the article or through supplementary data files.

INTRODUCTION

Integrons are genetic elements that facilitate horizontal gene transfer in Bacteria (Stokes & Hall, 1989), and Archaea (Ghaly *et al.*, 2022). They are ancient structures that have been involved in the evolution of bacterial genomes for hundreds of millions of years (Rowe-Magnus & Mazel, 2001). Functional integrons are composed of an integron-integrase gene (*intI*), an integron recombination site (*attI*), a promoter that drives the expression of the integrase (P_{int}) and generally also have a second promoter (P_c), oriented for expression of gene cassette array proteins (Hall & Collis, 1995, Mazel *et al.*, 1998, Escudero *et al.*, 2018).

Gene cassettes are mobile, non-replicating elements, which generally consist of an open reading frame (ORF) and an *attC* site. They exist as circular molecules when excised from a cassette array. Although cassettes generally consist of a single ORF, cassettes that have two ORFs or ORF-less cassettes with promoter activity have been observed (Michael & Labbate, 2010, Tansirichaiya *et al.*, 2019, Blanco *et al.*, 2024). The tyrosine recombinase IntI can capture circular cassettes and integrate them into the genome by mediating the recombination between *attC* and *attI* sites, forming arrays of 1 to 200+ gene cassettes. As well as mediating the insertion of cassettes, IntI can also excise cassettes from an array. Cassette arrays lacking an integrase are called CALIN (clusters of *attC* sites lacking integron-integrases) (Cury *et al.*, 2016), and can be mobilized *in trans* by a functional IntI.

Technically, integrons themselves are not mobile, whereas their gene cassette cargo is. Integron activity can facilitate horizontal gene cassette transfer between prokaryotes, contributing to the rapid evolution and genetic diversity of Bacteria and Archaea (Escudero

et al., 2018). Because DNA damage and nutrient starvation induce activity of the integron integrase via bacterial SOS and stringent responses (Guerin *et al.*, 2009, Cambray *et al.*, 2011, Strugeon *et al.*, 2016), acquisition of novel genetic functions is preferentially triggered during periods of environmental challenge. This provides a mechanism for adaptive innovation when survival pressures are highest.

Integrons have been extensively studied because of their role in the accumulation and dissemination of antibiotic resistance genes in clinical isolates (Gillings *et al.*, 2008, Hipólito *et al.*, 2023). However, integrons are also common in other environments such as marine environments (Pereira *et al.*, 2020), soil (Ghaly *et al.*, 2019), and the plant rhizoplane (Rajabal *et al.*, 2024), (Qi *et al.*, 2024). In these environments, the majority of gene cassettes remain functionally uncharacterised, but predicted functions encode extensive functional diversity including traits involved in microbe-host interactions (Gillings, 2014, Escudero *et al.*, 2018, Ghaly *et al.*, 2020).

Xanthomonas is a genus of Gram-negative bacteria in the class Gammaproteobacteria that contains pathogenic strains able to cause disease in more than 400 different plants. In common with other genera of plant pathogens, *Xanthomonas* also contains strains associated with plants, that do not cause disease symptoms (Vauterin *et al.*, 1996, Essakhi *et al.*, 2015, Garita-Cambronero *et al.*, 2017). *Xanthomonas* is a large genus that encompasses more than 35 species, which are subdivided into pathovars (Timilsina *et al.*, 2020).

Integrons have been described in some *Xanthomonas* isolates (Gillings *et al.*, 2005, Barionovi & Scortichini, 2006, Barionovi & Scortichini, 2008). Using PCR with site-specific primers annealing to the proximal part of *intI* and to the *attI* region, Gillings and colleagues screened 32 *Xanthomonas* strains representing 12 pathovars, and found that all the strains analysed had an integron. In all cases, *intI* was integrated downstream of the acid dehydratase gene, *ilvD*, however, the majority of integrase genes were predicted to be inactivated by frameshifts, stop codons, or large deletions. Groups of strains with the same deletions or stop codons/frameshifts in *intI* usually contained identical arrays of genes. There was no evidence of integrons generating diversity within pathovars but strong evidence for diversity between pathovars. With some minor exceptions, individual pathovars had distinct proximal gene cassette arrays, and every cassette identified was found only in one pathovar.

Complete genome sequences for hundreds of *Xanthomonas* isolates are now available, allowing for a systematic and detailed investigation of integrons in these important plant-associated bacteria. Here, we have examined the presence of integrons in all publicly available complete genomes of *Xanthomonas*, significantly expanding our knowledge of these elements, and showing how integrons have been a dynamic component during *Xanthomonas* genome evolution.

METHODS

Xanthomonas classification and phylogeny

Complete genomes of *Xanthomonas* were downloaded from the National Center for Biotechnology Information (NCBI) Database (NCBI txid: 338) (708 genomes, last accessed September 2024). Taxonomic classifications of the genomes was based on the Genome Taxonomy Database (GTDB) (Parks *et al.*, 2022) release 2.2.0 using GTDB-Tk v2.4.0 (Chaumeil *et al.*, 2022) (Table S1). The command classify_wf was used with default settings. GTDB-Tk first aligns 120 single-copy phylogenetic marker genes, then classifies each genome based on its placement into domain-specific reference trees (built from 47,899 prokaryote genomes), its relative evolutionary divergence, and average nucleotide identity to reference genomes in the GTDB. Two genomes (GCA_041228075.1 and GCA_002240395.1) did not belong to the *Xanthomonas* genus (*Luteibacter* and *Luteimonas*_D, respectively) and were removed from the dataset. The GTDB-Tk classification system does not strictly adhere to the traditional nomenclature of *Xanthomonas* strains, sometimes reassigning species. We use GTDB-Tk classification in order to use a standardised microbial taxonomy method based on genome phylogeny, and not to attempt to re-classify or rename isolates.

Phylogeny of the *Xanthomonas* genus was inferred using on the alignment of the 120 marker genes produced with the GTDB-Tk command classify_wf using GTDB-Tk command infer (default setting with --gamma) which uses FastTree 2.1 (Price *et al.*, 2010) to build an approximately-maximum-likelihood phylogenetic tree. The tree was rooted with GCA_041228075.1 (*Luteibacter*) then the tip was removed with the R package ape 5.8-1 (Paradis & Schliep, 2019). Single-species phylogeny was built using Realphy (Bertels *et al.*, 2014) which maps genomes to a series of reference genomes via bowtie2 2.0.0-beta7 (Langmead & Salzberg, 2012). From these, multiple sequence alignments are constructed and used to infer phylogenetic trees via PhyML 3.1 (Langmead & Salzberg, 2012). Trees are visualised using the ggtree 3.16 (Yu *et al.*, 2017) and ggtreeExtra 2.3 (Xu *et al.*, 2021) R packages.

Analysis of integrons

Integrons were identified with IntegronFinder 2.0.5 (Néron *et al.*, 2022) (parameters: --local-max --gbk --promoter-attI) (Table S1). Integron sequences with 5 kb up and downstream were extracted (fasta files deposited at https://github.com/EC-MQ/Xanthomonas_integrons) and annotated with Bakta (Schwengers *et al.*, 2021). Taxonomic origins of integron gene cassette recombination sites (*attC*s) were predicted using the script attC-taxa.sh (Ghaly *et al.*, 2021, Ghaly *et al.*, 2022). The *attC*-taxa pipeline (https://github.com/timghaly/attC-taxa) can detect *attC* sites that are conserved among one of 11 bacterial taxa, comprising: Alteromonadales, Methylococcales, Oceanospirillales,

Pseudomonadales, Vibrionales, Xanthomonadales, Acidobacteria, Cyanobacteria, Deltaproteobacteria, Planctomycetes and Spirochaetes.

IntI sequences identified by Integron Finder were aligned using PRANK (Löytynoja, 2013) run with default settings, the alignment was stripped of gaps with the goalign 'clean sites' command (Lemoine & Gascuel, 2021) and the tree inferred with FastTree 2.1 (Price *et al.*, 2010) using the generalized time-reversible model (--gtr).

We used multiple approaches to annotate the cassette-encoded proteins. Proteins were functionally annotated with eggNOG-mapper v2 (Huerta-Cepas *et al.*, 2019, Cantalapiedra *et al.*, 2021), executed in DIAMOND (Buchfink *et al.*, 2015) mode. Additionally, Foldseek (Van Kempen *et al.*, 2024) was used to create a protein structural database with the ProstT5 protein language model (Heinzinger *et al.*, 2024). The database was then used to perform structural alignment against the SwissProt database using a Foldseek search. Foldseek convertalis was used to convert the alignment database in a tab-delimited output, only functional annotations against the Swiss-Prot database with a coverage of 80% and an e-value < 0.001 were considered.

To identify genes involved in functions of ecological relevance (trace gas oxidation, carbon cycling, nitrogen cycling, sulphur cycling, phosphorus cycling, iron cycling, plant-microbe interactions, and osmotic stress tolerance) we used the *EcoFoldDB-annotate* pipeline (Ghaly *et al.*, 2025).

Plant growth-promoting traits were identified using the Plant Growth-Promoting Traits Prediction tool (PGPT-Pred) (Ashrafi *et al.*, 2022). SignalP V6.0 (Almagro Armenteros *et al.*, 2019) was used for signal peptide predictions as a marker for identifying transmembrane or secreted gene products. DefenseFinder (Tesson *et al.*, 2022) was used to detect known anti-phage systems.

Unique gene orthologues encoded by the cassettes and their distributions were identified with Proteinortho 6.0.22 (Klemm *et al.*, 2023) run with the -singles option.

To detect genes encoding type III secretion effectors (T3SE), we used a database of 66 previously characterized 66 *Xanthomonas* T3SE retrieved from the EuroXanth platform (Costa *et al.*, 2024) (Biessy *et al.*, 2025). T3SE in the cassettes were identified with Proteinortho v6.0.22 (Klemm *et al.*, 2023) by querying the curated effectors database against the amino acid sequences of the cassette-encoded genes.

Horizontal gene transfer events between species

Alfy 1.0.5 (Domazet-Lošo & Haubold, 2011) was used to guide the detection of the movement of cassettes between integron arrays. Alfy was run with the -M option, and selecting only matches with a *P* value <0.05 within a sliding window of 100 bp. Only arrays

sharing closest homology (recombination) with at least 10% of their sequence with an array harboured by a different species were considered. Horizontal gene transfer (HGT) events of cassettes were further filtered based on average nucleotide identity. FastANI 1.33 (Jain *et al.*, 2018) was run between the arrays and the whole genomes of the strains. To be considered a genuine HGT event, ANI identity between arrays needs to be >96% and the ANI between the genomes harbouring them to be <95%, with at least a 2% ANI difference between cassette and genome. Cytoscape (Shannon *et al.*, 2003) was then used to visualise the numbers of cassettes transferred between *Xanthomonas* species.

RESULTS AND DISCUSSION

The *Xanthomonas* integron platform is ancestral

Xanthomonas complete genomes classified based on the Genome Taxonomy Database (GTDB) as "*Xanthomonas*" (n=629) and "*Xanthomonas_A*" (n=78), known also as *Xanthomonas* group 2 and 1, respectively (Pena *et al.*, 2024) were analysed for integron features. We retained the genomes of *Xanthomonas_A,* even though they are classified as a different genus by GTDB-Tk, because from a plant pathology perspective they are still considered *Xanthomonas*, and encompass *X. translucens,* an important causal agent of diseases in cereal crops and forage grasses (Sapkota *et al.*, 2020).

Using IntegronFinder 2.0.5 (Néron *et al.*, 2022), we identified integrons, In0 (integron-integrases that lack cassettes), or CALINs (clusters of *attC* sites lacking integron-integrases) in 93% of the genomes (657 genomes) (Figure 1). *X. albilineans* (n=6, group 1) and *X. fragariae* (n=6, group 2) were the only species with more than 2 genome sequences available that did not harbour either an *intI* or *attC* sites. However, integrons have been previously detected in some isolates of *X. fragariae* via PCR amplification (Barionovi & Scortichini, 2006).

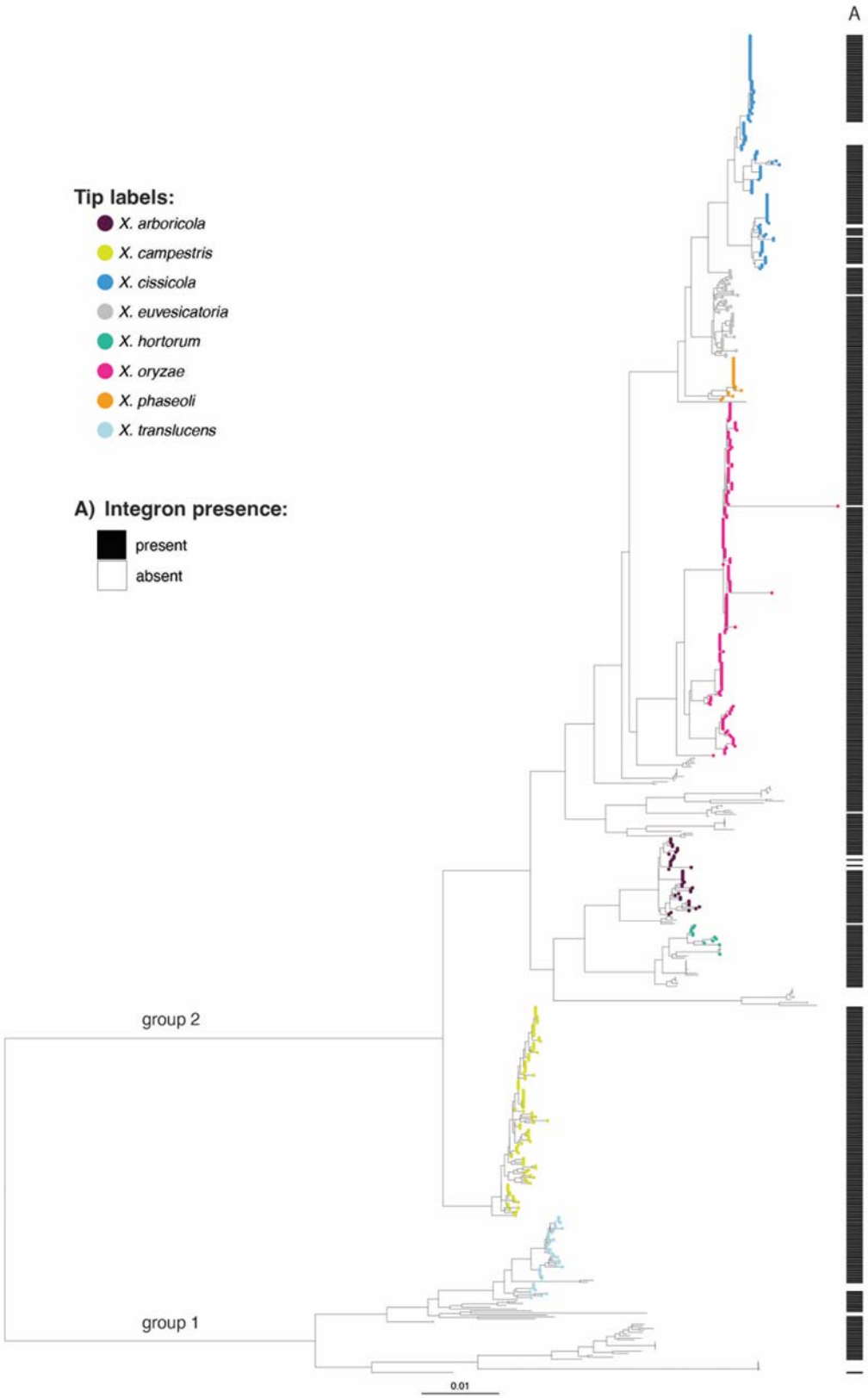

210

211 **Figure 1 – Distribution of integron platforms in *Xanthomonas* groups 1 and 2.** The maximum likelihood
212 phylogenetic tree is based on a concatenated alignment of 120 top-ranked marker proteins. The tree was

rooted at the midpoint. Tips are labelled with species names assigned with Genome Taxonomy Database phylogeny. Integrons were classified as present if the isolates carried a functional integron, *intI* only or an *attC* array only. Scale bar indicates substitutions per site.

Because integrons are widespread in *Xanthomonas*, our first question was whether the acquisition of the integron module was ancestral. The integron-integrase encoding gene *intI* was integrated downstream *ilvD* in all genomes, with the two exceptions being isolates of *X. oryzae* and *X. cucurbitae*. Of the 187 *oryzae* isolates examined, *X. oryzae* pv. *oryzicola* (26 genomes) harbour a truncated *intI* (561 bp) that was not integrated downstream *ilvD.* However, the integron locus (*intI* and cassette array) is surrounded by transposases, which could indicate that the integron was moved via transposition. In all seven *X. cucurbitae* genomes, *intI* was not integrated downstream *ilvD.* However, downstream of *ilvD* there are two genes without recognizable *attCs* which are encoded in the other integrons (including a DUF1488 encoding gene which occurs in multiple species).

The different genomic locations of *intI* could be explained by either within-genome transposition or recombination (*intI* was initially located downstream *ilvD* and then moved), or by an independent acquisition of *intI* from another source which was integrated in a different locus. To test this, we constructed the phylogeny of all the *Xanthomonas intIs* (Figure S1). If *intIs* located elsewhere from *ilvD* were acquired independently, they would likely have a different evolutionary history, and form separate clades in the *intI* phylogeny.

The phylogeny of *intI* clusters this gene within species, generally being independent of the integration locus. *X. oryzae intIs* cluster together, and the *X. cucurbitae intIs* form a clade with pv. *phaseoli* (Figure S1). The only notable exception is *X. arboricola*. *X. arboricola* strains can carry one of two variant *intIs*. In two strains, *intI* clusters closest to the *X. campestris intIs* and are truncated and likely not functional. Phylogenetically close *X. arboricola* strains do not harbour an *intI* at all. The other *X. arboricola* strains carry *intI* (either full-length or with an early stop codon) that are more distantly related to all other *intIs*. These more distantly related *intI* could have been acquired from a source outside *Xanthomonas*. We compared the *ilvD-intI* locus sequence in two representative *arboricola* strains harbouring the two *intI* variants (GCA_018141705.1 and GCA_905367745.1). While the *ilvD* genes share 97.1% average nucleotide identity (ANI), the *intIs* share 68.2% ANI, suggesting a recombination event.

We used two full length *intI* variants (one belonging to *X. arboricola*, one to *X. campestris*) as a query in a BLASTn search on complete genomes in NCBI excluding *Xanthomonas* (taxid:338). The two closest *intI*s belonged to *Lysobacter* sp. CECT 30171 (locus tag: LYB30171_00805) and *[Pseudomonas] boreopolis* strain GO2 (locus tag: M3M27_18655) (both genera in the Xanthodomonaceae family). Curiously, in isolate GO2, *intI* was also located downstream of *ilvD*. We constructed a phylogenetic tree using *Xanthomonas intI*

sequences longer than 900 bp and included the *intIs* of CECT 30171 and GO2, using *Vibrio* sp. SCSIO 43136 *intI* as an outgroup (Figure 2). The *intI* variants in *X. arboricola* were more closely related to the *intI* in GO2 than the other *Xanthomonas intIs*. *ilvD* phylogeny instead clusters together all *X. arboricola* isolates within the *Xanthomonas* group 2, and GO2 as basal both to *Xanthomonas* group 1 and 2 isolates. This suggests that, in those *arboricola* strains, *intI* was acquired via horizontal gene transfer (HGT) from another member of the Xanthodomonaceae family.

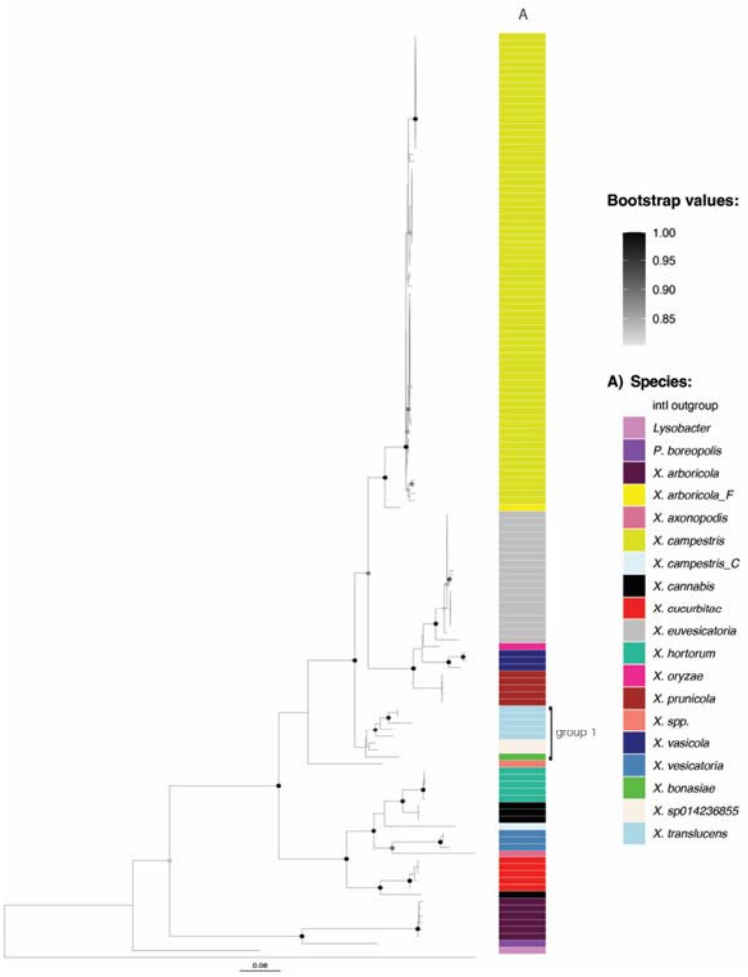

Figure 2 – Phylogeny of *intI*. Sequences of *intI* longer than 900 bp were aligned with PRANK, stripped of gaps and used to infer the tree with FastTree. *IntI* from *Vibrio* sp. SCSIO 43136 (locus tag: J4N39_08275) was used as an outgroup. The scale bar indicates substitutions per site. Only bootstrap values 0.80 are shown. Group 1 *Xanthomonas* are indicated on the side of the plot.

ilvDs of *Xanthomanas* group 1 form a separate group in comparison to group 2 (Figure S2), while the group 1 *intIs* are nested within the most common *Xanthomanas intIs*. Genetic exchange between a restricted number of strains of group 2 and the entire group 1 clade has been reported (Pena *et al.*, 2024), therefore it is plausible that horizontal transfer of an

intI gene from a group 2 *Xanthomonas* species occurred during the early evolutionary history of group 1 *Xanthomonas*.

Together, this suggests that the acquisition of the integron platform was ancestral to the *Xanthomonas* genus, and then *intI* diversified with the species. The exceptions are some *X. arboricola* strains that could have recruited *intI* from another source, while group 1 *Xanthomonas* could have acquired *intI* from group 2 *Xanthomonas* in one single gene flow event.

Additionally, approximately 50% of genomes harbor CALINs, here defined as clusters of at least two *attC* sites, in loci other than the canonical *ilvD* region and in the absence of a proximal *intI* gene. In genomes where *intI* is retained, this gene is consistently integrated downstream of *ilvD,* while these CALINs show spatial separation, being located in other regions of the genome. Among the species represented by more than 10 genomes, CALINs not adjacent to *ilvD* were identified at seven distinct chromosomal loci. In *X. arboricola*, *campestris*, *cissicola*, *euvesicatoria*, and *hortorum*, CALINs consistently occurred adjacent to *lamG* and/or *secF*. In *X. cissicola*, additional CALINs were located near *recD* and a gene encoding a NAD(P)/FAD-dependent oxidoreductase. In *X. oryzae*, two strains possessed CALINs adjacent to an outer membrane protein gene, while in *X. translucens*, CALINs were observed at two distinct genomic positions. One *X. campestris* strain (GCA_028749605.1) harboured a CALIN on a conjugative plasmid. The relatively conserved positioning of CALINs across species supports the hypothesis of ancestral integron activity. This contrasts with experimental data from *Escherichia coli*, where cassette libraries integrated via *attG* sites (consensus recombination sequences that are not *attC* or *attI*) exhibited a broad distribution across numerous genomic loci, indicating that *de novo* integration is typically less site-specific (Loot *et al.*, 2024).

Acquisition of the integron platform is ancestral but its activity is progressively lost

To investigate integron integrase activity and the complement of integron gene cassettes in *Xanthomonas* genomes, we focused on species which had more than 10 genomes in our dataset: *campestris* (n=111) (Figure 3), *cissicola* (n= 124) (Figure 4), *arboricola* (n=41) (Figure S3), *translucens* (n=46) (Figure S4), *euvesicatoria* (n=46) (Figure S5), *oryzae* (n=161) (Figure S6), *phaseoli* (n=23) (Figure S7), *hortorum* (n=12) (Figure S8). A detailed description of the integrons in these eight species is reported in the Supplementary Results Section.

Although integron associated sequences are common in *Xanthomonas* groups 1 and 2, most strains appear to have lost integron integrase activity, and the distribution of functional integrons appears to be species specific. However, among the species analysed, *X. campestris* stands out for maintaining a largely functional integron platform (Figure 3). A high proportion (85.6%) of its genomes carry a full-length *intI* gene, and integrons are

consistently flanked by extensive cassette arrays (ranging from 3 to 29 *attCs*, averaging 14.3 per genome). Cassette composition is highly variable even among strains of the same pathovar, suggesting that, in *X. campestris*, integron activity drives rapid diversification within genetically related groups. This robust activity is also evident in the gene content: 216 orthologous cassette-encoded genes were identified, 41.1% of which are singletons (observed in only one instance in this dataset). Despite this extensive variability, a gene encoding a DUF1488 domain-containing protein is present in the cassettes of 81.5% of genomes, while *symE* (a toxin-encoding gene) is found in 56.8% of the cassette arrays. This level of integron retention suggests that active integrons continue to play a key role in the adaptive evolution of *X. campestris*.

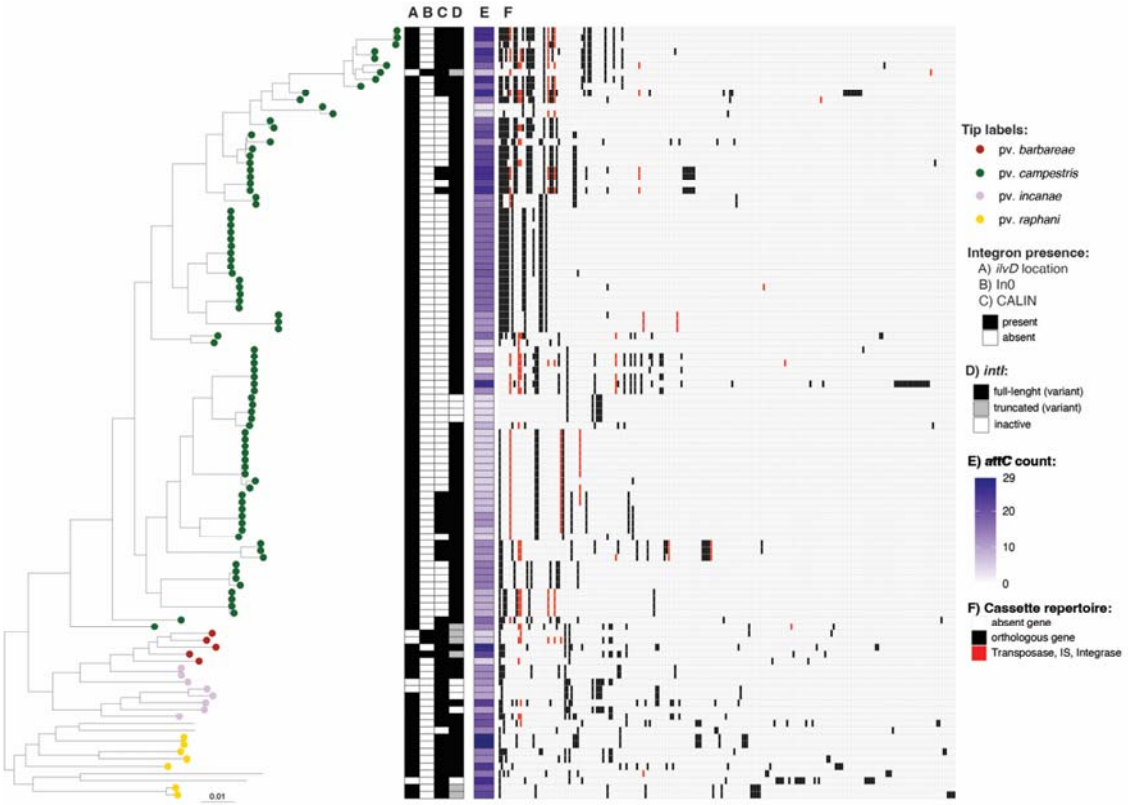

Figure 3 – Integrons in *X. campestris*. The phylogeny of *X. campestris* was built using Realphy, using GCA_000007145.1 as a reference genome. The tree was rooted with GCA_000972745 (*X. arboricola*) then the tip was removed from the tree. Tip labels show pathovars. The scale bar indicates substitutions per site. A) Indicates the presence of a complete integron or *attC* sites in the *ilvD* locus, B) indicates the presence of *intI*, C) indicates the presence of a CALINs (cluster of *attC* sites) not in the ilvD locus. D) indicates whether IntI is predicted to be functional (full length). E) indicates the number of *attC* sites (number of cassettes) in the genome. Panel F) represents the distribution of orthologous genes among all cassettes carried by the corresponding isolate inferred with Proteinortho. Orthologous genes are listed in decreasing order based on the number of strains within the species that carry them.

X. arboricola exhibited a modest preservation of the *intI* gene with 7% of strains retaining a full-length *intI*. In the remaining genomes, *intI* is either deleted or contains an early stop

327 codon. The *X. arboricola* phylogeny divides strains into two clades, clade A which includes
328 pathovars that cause diseases in *Prunus*, *Juglans*, and *Corylus* spp. (pvs. *pruni*, *juglandis*, and
329 *corylina*, respectively), and clade B which comprises many isolates lacking metadata (Figure
330 S3). Among clade A isolates, none possess a full-length *intI.* In contrast, clade B strains that
331 carry *intI*, either full-length or truncated (accounting for 58.8% of clade B isolates), harbor a
332 variant likely acquired via HGT, suggesting the acquisition event dated prior to the
333 diversification of this clade. Strains of clade B also carried more cassettes and a broader
334 array of genes compared to clade A.

335 *X. translucens* (Figure S4) and *X. euvesicatoria* (Figure S5) emphasize the dynamic nature of
336 integrons in *Xanthomonas.* Both species exhibit high frequencies of full-length *intI* (22.7%
337 and 45.6% respectively) and variability in cassette content is high (44.6% and 50%
338 respectively).

339 *X. oryzae* includes pathogens of rice (pv. *oryzae* and pv. *oryzicola*), and pathogens of a
340 pervasive weed species that grows along rivers and canals surrounding rice paddies (pv.
341 *leersiae*). However, only X11-5A, a weakly pathogenic strain (Triplett *et al.*, 2011) distantly
342 related to the above-mentioned pathovars carries a full-length *intI*. Divergent cassette
343 compositions were observed among the pathovars (Figure S6). This supports the hypothesis
344 that integron activity in *X. oryzae* was ancestrally active, followed by progressive
345 inactivation concomitant with pathovar diversification.

346 None of the *X. cissicola* (Figure 4) and X. *phaseoli* (Figure S7) isolates retain a full-length,
347 functional *intI*. However, 28.7% and 38% of the genes carried by the cassettes in these
348 species, respectively, appear in one isolate only (singletons). *X. cissicola* comprises isolates
349 commonly known as *X. citri*, an important pathogen able to infect many plants including
350 *Citrus* (pv. *citri*). *X. citri* pv. *citri* includes three recognized pathotypes: A, A*, and AwA. All
351 pv. *citri* genomes analysed here, which include both A and AwA pathotypes, harbor a CALIN
352 element adjacent to *secD* and lack the integrase gene *intI*. All the CALINs in the pv. *citri*
353 contain the same two gene cassettes, which are not present in any other genome analysed
354 in this study, suggesting that the integron platform was inactivated prior to pathotype
355 diversification (Figure 4). A recent genomic study of 95 pv. *citri* strains estimated that the
356 diversification of these pathotypes occurred 1,730 to 5,663 years ago (Patané *et al.*, 2019).
357 Given that citrus domestication is thought to have occurred at least 2,000 years ago (Rao *et*
358 *al.*, 2021), the inactivation event likely predates the domestication of the host genus. One of
359 the two cassettes encodes a protein homologous to members of the late embryogenesis
360 abundant (LEA) protein family, which is known to confer protection against water deficit in
361 bacteria (Raga-Carbajal *et al.*, 2022). This indicates that the cassette's function could be
362 oriented toward general environmental stress rather than mediating specific interactions
363 with the plant host.

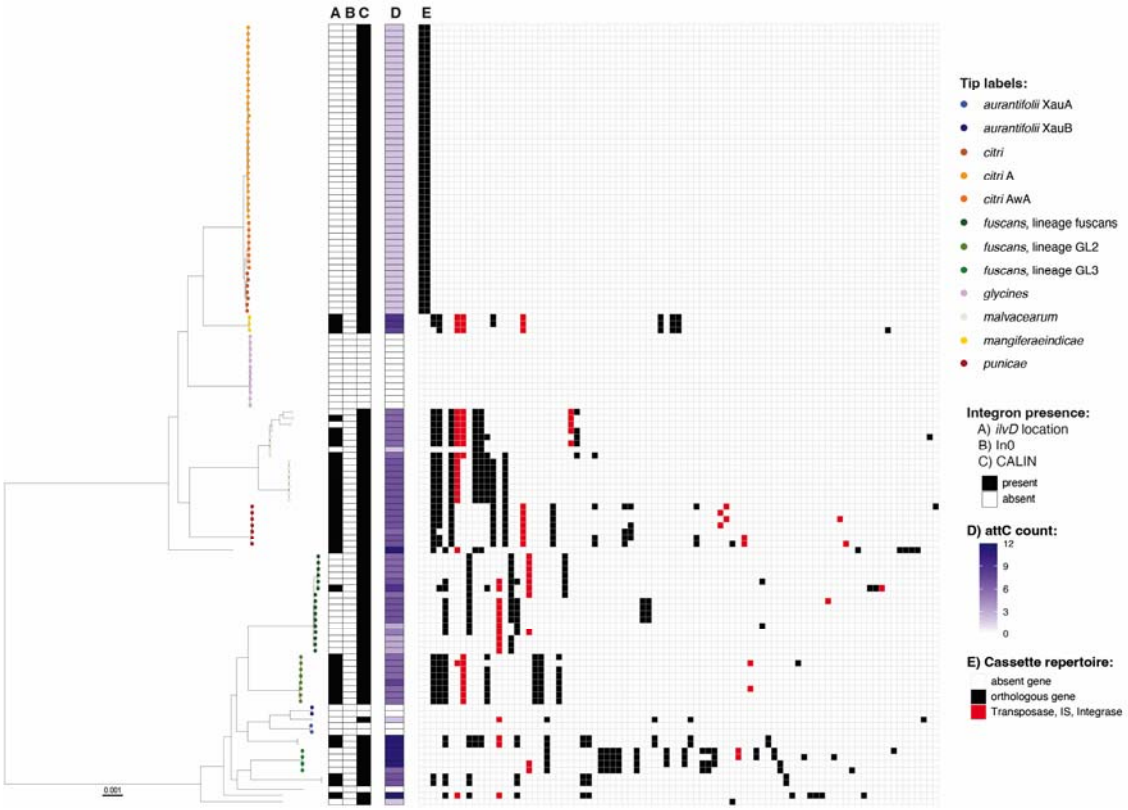

Figure 4 – Integrons in *X. cissicola*. The phylogeny of *X. cissicola* was built using Realphy, using GCA_000007165.1 as a reference genome. The tree was rooted with GCA_000009165.1 (*X. euvesicatoria*) then the tip was removed from the tree. Tip labels show pathovars, which were assigned from the literature search. The scale bar indicates substitutions per site. A) Indicates the presence of a complete integron or *attC* sites in the *ilvD* locus, B) indicates the presence of *intI*, C) indicates the presence of a CALINs (cluster of *attC* sites) not in the ilvD locus. D) indicates the number of *attC* sites (number of cassettes) in the genome. Panel E) represents the distribution of orthologous genes among the all the cassettes carried by the corresponding isolate inferred with Proteinortho. Orthologous genes are given in decreasing order based on the number of strains within the species that carry them.

Gene cassette abundance is species specific.

We investigated whether variation in integron cassette array size, quantified by the number of *attC* sites per genome, is primarily shaped by the host genetic background (i.e., *Xanthomonas* species) or by the ecological context of isolation, categorized by cultivation type (crop, non-crop, crop tree, or ornamental host plants). We used only the species that had more than 10 genomes in our dataset, additionally, we excluded genomes lacking information on the host of isolation, and a strain isolated from mud. We performed a Kruskal-Wallis test to assess if there were statistically significant differences in *attC* number associated with bacterial species and the type of plant the strains were isolated from. The

results showed significant variation in *attC* count across both factors (Figure S9). Regarding the cultivation type, the average mean was 12.1 *attC*s for ornamental, 9.77 for non-crop, 6.01 for crop and 3.05 for tree crop. Dunn's test with Bonferroni adjustment showed statistically significant ($p<0.001$) differences between strains isolated from crops and non-crops, between crops and ornamentals, non-crop and tree crops and between ornamentals and tree-crops. Dunn's test identified three distinct statistical groupings among the *Xanthomonas* species, with *X. oryzae* and *X. phaseoli* forming the group with the fewest cassettes, and *X. campestris* having the highest number.

To assess the contribution of species identity and cultivation type on variation in cassette number (number of *attC* sites) across samples, we performed a PERMANOVA analysis. The results indicated that cultivation explained 8.78% of the variation in number of *attC* sites (p-value = 0.001), suggesting that the type of cultivation has a significant, though relatively small, effect on the observed variation. In contrast, the species the isolate belong to accounted for a much larger proportion, explaining 48.17% of the variation (p-value = 0.001). This highlights the significant role of taxonomy at the species level in shaping the number of *attC* sites, with its influence being far more pronounced than that of cultivation.

Cassette arrays in *Xanthomonas* harbor diverse but poorly characterized gene functions

Prediction of the taxonomic origins of integron *attC*s was performed with a classification tool developed for *attC*s, which uses both sequence and structural homology information (Ghaly *et al.*, 2021), to identify matches to known *attC* 'types'. The method classified all *attC* sites in the *Xanthomonas* strains analysed as originating within the *Xanthomonadales*. Therefore, there is no evidence of long-distance acquisition of cassettes, and the cassettes appear to circulate at least within the *Xanthomonadales* family.

Arrays greatly varied greatly in length across genomes, with a maximum of 46 cassettes in a single genome (X. *arboricola_F* GCA_040182365.1) and 33 cassettes in a single array (X. *arboricola* GCA_041475745.1 and GCA_041475785.1) (Table S1). Despite the majority of the isolates carrying inactive integron modules, with *intI* deleted or truncated, the cassette arrays appear to have been extremely dynamic before the inactivation of the integron integrase.

Overall, the 706 *Xanthomonas* genomes carried 1004 cassettes arrays, with a total of 4,773 cassettes, within these, Proteinortho (Klemm *et al.*, 2023) identified 1,087 different orthologous genes. Of the 1,087 orthologous genes identified by Proteinortho, 476 (43.8%) were present as singletons, unique to one isolate.

Of the 1,087 orthologous genes, only 11.9% could be classified into a known Clusters of Orthologous Groups of proteins (COG) category (Galperin *et al.*, 2025). This

421 underrepresentation of known COGs among cassette proteins is well known (Rowe-Magnus
422 *et al.*, 2003, Mazel, 2006, Boucher *et al.*, 2007, Ghaly *et al.*, 2024, Rajabal *et al.*, 2024). Of
423 the most represented functions, excluding unknown and recombination and repair, 1.47%
424 of the protein had a putative role in transcription, 0.9% in amino acid transport and
425 metabolism, and 0.55% in defence mechanisms. To gain further insight into possible
426 cassette functions, we performed both sequence-based homology searching against
427 eggNOG 5.0 (Huerta-Cepas *et al.*, 2019), and protein structural homology searching against
428 the Swiss-Prot database. From this combined approach, putative functions could only be
429 assigned to 6.8% of the proteins. Of these annotated cassette-encoded proteins, 47.7%
430 were classified either as transposase, integrases or insertion sequences (4.8% of the total).
431 The presence of insertion sequences and transposases within gene cassettes (Ghaly *et al.*,
432 2024), and targeting *attC* sites (Tetu & Holmes, 2008, Post & Hall, 2009), has been
433 frequently observed in past integron studies.

434 Signal peptides were identified in 11.6% of cassette-encoded proteins, using signalP6.0
435 (Teufel *et al.*, 2022). Again, transmembrane and secreted proteins are commonly encoded
436 by gene cassettes in Bacteria (Rowe-Magnus *et al.*, 2003, Ghaly *et al.*, 2023) and are
437 hypothesized to help facilitate interactions with their broader environment. Additionally,
438 PGPT-Pred (Ashrafi *et al.*, 2022) predicted 6.7% of cassette-encoded proteins to have plant
439 growth promoting traits such as biofertilization, plant signal production and stress control.
440 However, the most common category, at 4.9% of the total proteins, were categorised to
441 have competitive exclusion functions. These included antimicrobial resistance and
442 detoxification functions, and toxin-antitoxin systems, which in a plant pathogenic context
443 could contribute to niche adaptation by enhancing survival in a competitive microbial
444 environment. One gene was classified by the EcoFoldDB (Ghaly *et al.*, 2025) pipeline as
445 involved in spermidine production, which can play an important role in plant growth and
446 stress (Dunn & Becerra-Rivera, 2023).

447 DefenseFinder (Tesson *et al.*, 2022) identified 20 orthologous genes (1.8%) as genes
448 involved in defences against phages. Twelve different defence systems were detected, these
449 included restriction-modification and abortive infection systems, but also the newly
450 described Kiwa (Zhang *et al.*, 2023) and Shedu defence systems (Loeff *et al.*, 2025).

451 Using a database of previously characterized type three secretion system effectors (T3SEs)
452 retrieved from the EuroXanth platform (Costa *et al.*, 2024, Biessy *et al.*, 2025), we identified
453 two T3SEs: AvrBs3 (a Transcription Activator-Like effector, TALe) in African-like pv. *oryzae*
454 (Schepler-Luu *et al.*, 2023), and XopAF2 in three *X. vasicola* isolates. T3SEs are protein
455 secreted via the type III secretion system (T3SS) that suppress or induce plant defences.
456 TALes are a particular type of T3SE, once inside the host cell, they translocate to the nucleus
457 where their unique domain of tandemly arranged 34-amino acid repeats mediates binding
458 to specific promoter elements. Several TALes are known to induce host SWEET sucrose
459 uniporter genes, thereby facilitating sucrose efflux from xylem parenchyma into the

460 apoplasm at the infection sites. TALes may enhance disease by targeting susceptibility
461 genes, or may trigger a resistance response, and are therefore important for pathogen host
462 range and virulence (Schepler-Luu *et al.*, 2023).

463 Given that the majority of cassette-encoded proteins are of unknown function and often
464 occur as singletons (observed only in one strain), the phenotypic impact of these cassettes
465 remains unclear. It is uncertain whether they confer a selective advantage or are maintained
466 in the arrays through neutral processes. A cassette that is conserved across multiple species
467 is more likely to encode a beneficial function. The most widespread cassette, identified in 13
468 species, encodes *symE* and the non-coding small RNA *sRNA-Xcc1*. *sRNA-Xcc1* is known to be
469 activated by regulatory elements of the T3SS (Chen *et al.*, 2011), suggesting a potential role
470 in plant host colonization. In *E. coli*, *symE* forms part of the SymE-SymR toxin-antitoxin
471 system, where SymE induces nucleoid condensation, disrupts DNA replication and
472 transcription, and causes double-strand DNA breaks (Thompson *et al.*, 2022). Regulation in
473 *E. coli* occurs via the cis-encoded small RNA *SymR* (Kawano *et al.*, 2007), whereas in the
474 integron cassettes, *sRNA-Xcc1* is located upstream of *symE*, suggesting a divergent
475 regulatory mechanism. Notably, unlike most integron-associated genes oriented to be
476 transcribed from the *Pc* promoter (typically located within *intI*), both *sRNA-Xcc1* and *symE*
477 are oriented in the opposite direction and not under *Pc* control.

478 Excluding transposases, the second most recurrent cassette, shared among 8 species,
479 encoded a protein of unknown function. The third most recurrent, present in 7 species,
480 included two hypothetical proteins and a gene conferring resistance to bleomycin.
481 Bleomycin resistance genes have been previously identified as enriched in gene cassettes
482 relative to total metagenomes in environmental samples, as shown by both cassette-
483 targeted amplicon sequencing and shotgun metagenomics (Ghaly *et al.*, 2023). One of the
484 recurring cassettes is an "empty" cassette which can occur multiple times in the same array.
485 This cassette could have promoter activity as it was previously suggested in other species
486 (Michael & Labbate, 2010, Tansirichaiya *et al.*, 2019, Blanco *et al.*, 2024).

487

488 **Detection of inter-species horizontal transfer of cassette arrays**

489 To assess interspecies cassette gene sharing, we examined pairs of species that most
490 frequently share orthologous genes. As expected, species harbouring a greater number of
491 cassettes tend to share more orthologous genes with others. For example, *X. arboricola* and
492 *X. campestris* shared the highest number of orthologous genes (21), with *X. campestris*
493 sharing the most overall (57 orthologous genes across multiple species).

494 Orthologous genes encoded in the cassettes are shared between *Xanthomonas* species and
495 even between group 1 and 2 *Xanthomonas*. We then looked for more recent evidence of
496 HGT of cassettes present in multiple species. We used Alfy v1.0.5 (Domazet-Lošo & Haubold,

2011) to identify putative regions subject to HGT, selecting those based on the difference in ANI between the cassette and the genomes harbouring them. With this approach, we detected the movement of 95 cassettes between 38 pairs of species (Figure 5). The highest flux of cassettes (10) was between *X. arboricola* and *euroxanthea,* and between *X. campestris* and *X. hortorum*. However, *X. campestris* is the species with the highest flux of cassettes compared to any other species (36). One of the cassettes that showed evidence of horizontal transfer was that carrying *symE* and *sRNA-Xcc1*.

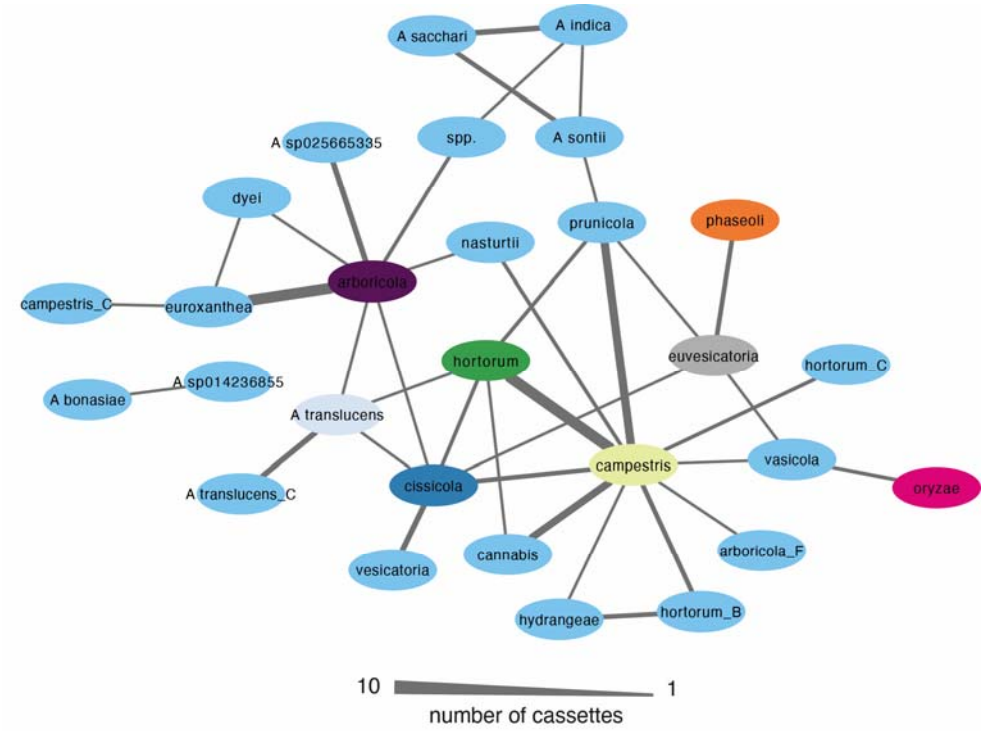

Figure 5 – Horizontal transfer of cassettes among *Xanthomonas* species. Cytoscape network illustrating transfer of cassettes between species. Nodes represent *Xanthomonas* species, species containing more than 10 genomes in the dataset are coloured as in Figure 1 (tip labels). Line width between species is proportional to the number of cassettes moved between species.

CONCLUSIONS

Our comprehensive analysis of 706 complete genomes reveals that the acquisition of the integron platform is likely an ancestral event in the evolution of the *Xanthomonas* genus. The widespread conservation of the *intI* gene downstream of *ilvD* across species, along with *intI* phylogeny, strongly supports the early acquisition of this mobile genetic element. Only in *X. arboricola* clade B, the "original" *intI* appears to have been substituted via HGT with an *intI* from another member of the Xanthodomonaceae family.

Despite the ancestral acquisition, our results show that integron activity, defined by the presence of full length, potentially functional *intI* genes, and large and diverse cassette arrays, has been progressively lost in many *Xanthomonas* lineages. This inactivation appears to be species-specific and often predates major evolutionary or ecological transitions, such as pathovar diversification, such as in *X. cissicola* and *X. oryzae*. Nevertheless, in species such as *X. campestris*, integrons remain robustly functional and continue to contribute to genomic diversification, as evidenced by the presence of full length *intI*, high cassette variability, and the of strain specific gene cassettes in cassette arrays. Selective pressures and ecological niches may favor the retention of an active integron system in this species and not in the others, for reasons not clear at this time.

The phenotypic impact of the large pool of gene cassettes residing in *Xanthomonas* genomes remains largely unresolved. Nearly half of orthologous genes carried by gene cassettes occurred only once, contributing to strain level genetic variability. These rare genes may represent a reservoir of adaptive potential, but could also be selectively neutral or even transient. Cassettes in *Vibrio* chromosomal integron platforms have been suggested to have been selected to be as neutral as possible (Blanco *et al.*, 2024). The frequent occurrence of hypothetical proteins, including highly conserved cassettes ORFs, suggests important functional roles that remain undiscovered. For instance, a cassette carrying the DUF1488 encoding gene is present, a few times in multiple copies, in 16.7% of the genomes across 6 species, sometimes with multiple copies within the same integron array. Among cassette-encoded genes with predicted putative functions, many have predicted functions linked to environmental interaction and thus have the potential to contribute to niche adaptation. For example, the most widespread cassette in our dataset encodes *symE* and the small coding sRNA-Xcc1, known to be activated by T3SS regulatory proteins (Chen *et al.*, 2011), which may influence bacterial growth during plant colonization. In *Xanthomonas*, we found a fairly small fraction of cassette genes to be classified as involved defence mechanisms, despite the emerging role of integron platforms in encoding anti-phage genes (Darracq *et al.*, 2025, Getz *et al.*, 2025, Kieffer *et al.*, 2025). However, this may be an underestimate, as work on large sedentary chromosomal integrons in *Vibrio cholerae* showed that 20% of their cassettes with no predicted function encode for anti-phage defence systems, despite these genes not being detected as such by bioinformatic tools (Darracq *et al.*, 2025).

Importantly, our analysis revealed evidence of interspecies horizontal transfer of cassettes. For both *X. campestris* and *X. arboricola* there is evidence of recent horizontal transfer of integron-associated cassettes with other *Xanthomonas* species. Interestingly, however, despite their high levels of cassette acquisition, there is little evidence of recent and direct cassette exchange between these two species. Instead, *X. campestris* shows the highest degree of gene sharing with *X. hortorum*, a species more closely related to *X. arboricola* than to *X. campestris*. Conversely, the species with which *X. arboricola* shares the greatest number of cassettes is *X. euroxanthea*, its closest phylogenetic neighbour among the

genomes analysed. These patterns suggest that both phylogenetic proximity and ecological overlap, such as co-occurrence in the phyllosphere or endosphere during mixed infections, have contributed to the dynamics of cassette exchange. The shared habitat provides repeated opportunities for interspecies contact and genetic exchange, likely promoting the horizontal dissemination of integron cassettes across the genus.

In summary, our analysis indicates that integron platforms were likely acquired early in the evolution of the *Xanthomonas* genus and have since followed divergent evolutionary trajectories. While many lineages show signs of integron inactivation, others, such as *X. campestris*, retain active systems contributing to genomic diversification. The gene cassettes carried by these integrons, including many with unknown or potentially adaptive functions, add to strain-level variability and may influence niche adaptation. Patterns of horizontal gene transfer suggest that both phylogenetic relatedness and ecological overlap shape cassette exchange across species, highlighting integrons as dynamic elements in the evolutionary landscape of *Xanthomonas*.

Funding information: This work is supported by funding from the ARC Centre of Excellence in Synthetic Biology (CE200100029).
Conflicts of interest: The authors declare that there is no conflict of interest.

REFERENCES

Almagro Armenteros JJ, Tsirigos KD, Sønderby CK, Petersen TN, Winther O, Brunak S, von Heijne G & Nielsen H (2019) SignalP 5.0 improves signal peptide predictions using deep neural networks. *Nature biotechnology* **37**: 420-423.

Ashrafi S, Kuzmanović N, Patz S, Lohwasser U, Bunk B, Spröer C, Lorenz M, Elhady A, Frühling A & Neumann-Schaal M (2022) Two new Rhizobiales species isolated from root nodules of common sainfoin (*Onobrychis viciifolia*) show different plant colonization strategies. *Microbiology Spectrum* **10**: e01099-01022.

Barionovi D & Scortichini M (2006) Assessment of integron gene cassette arrays in strains of *Xanthomonas fragariae* and *X. arboricola* pvs. *fragariae* and *pruni*. *Journal of Plant Pathology* 279-284.

591 Barionovi D & Scortichini M (2008) Integron variability in *Xanthomonas arboricola* pv.
592 *juglandis* and *Xanthomonas arboricola* pv. *pruni* strains. *FEMS microbiology letters* **288**: 19-
593 24.

594 Bertels F, Silander OK, Pachkov M, Rainey PB & Van Nimwegen E (2014) Automated
595 reconstruction of whole-genome phylogenies from short-sequence reads. *Molecular biology*
596 *and evolution* **31**: 1077-1088.

597 Biessy A, Cadieux M, Ciotola M, McDuff F, Soufiane B, Laforest M & Filion M (2025)
598 Characterization of a plant-pathogenic T3SS-lacking *Xanthomonas* strain isolated from
599 common ragweed. *Plant Pathology* **74**: 308-319.

600 Blanco P, Hipólito A, García-Pastor L, Trigo da Roza F, Toribio-Celestino L, Ortega AC, Vergara
601 E, San Millán Á & Escudero JA (2024) Identification of promoter activity in gene-less
602 cassettes from *Vibrionaceae* superintegrons. *Nucleic acids research* **52**: 2961-2976.

603 Boucher Y, Labbate M, Koenig JE & Stokes H (2007) Integrons: mobilizable platforms that
604 promote genetic diversity in bacteria. *Trends in microbiology* **15**: 301-309.

605 Buchfink B, Xie C & Huson DH (2015) Fast and sensitive protein alignment using DIAMOND.
606 *Nature methods* **12**: 59-60.

607 Cambray G, Sanchez-Alberola N, Campoy S, Guerin É, Da Re S, González-Zorn B, Ploy M-C,
608 Barbé J, Mazel D & Erill I (2011) Prevalence of SOS-mediated control of integron integrase
609 expression as an adaptive trait of chromosomal and mobile integrons. *Mobile DNA* **2**: 6.

610 Cantalapiedra CP, Hernández-Plaza A, Letunic I, Bork P & Huerta-Cepas J (2021) eggNOG-
611 mapper v2: functional annotation, orthology assignments, and domain prediction at the
612 metagenomic scale. *Molecular biology and evolution* **38**: 5825-5829.

613 Chaumeil P-A, Mussig AJ, Hugenholtz P & Parks DH (2022) GTDB-Tk v2: memory friendly
614 classification with the genome taxonomy database. *Bioinformatics* **38**: 5315-5316.

615 Chen X-L, Tang D-J, Jiang R-P, He Y-Q, Jiang B-L, Lu G-T & Tang J-L (2011) *sRNA-Xcc1*, an
616 integron-encoded transposon-and plasmid-transferred trans-acting sRNA, is under the
617 positive control of the key virulence regulators HrpG and HrpX of *Xanthomonas campestris*
618 pathovar *campestris*. *RNA biology* **8**: 947-953.

619 Costa J, Pothier JF, Bosis E, Boch J, Kölliker R & Koebnik R (2024) A community-curated
620 DokuWiki resource on diagnostics, diversity, pathogenicity, and genetic control of
621 xanthomonads. *Molecular Plant-Microbe Interactions* **37**: 347-353.

622 Cury J, Jové T, Touchon M, Néron B & Rocha EP (2016) Identification and analysis of
623 integrons and cassette arrays in bacterial genomes. *Nucleic acids research* **44**: 4539-4550.

624 Darracq B, Littner E, Brunie M, Bos J, Kaminski PA, Depardieu F, Slesak W, Debatisse K,
625 Touchon M & Bernheim A (2025) Sedentary chromosomal integrons as biobanks of bacterial
626 antiphage defense systems. *Science* **388**: eads0768.

627 Domazet-Lošo M & Haubold B (2011) Alignment-free detection of local similarity among
628 viral and bacterial genomes. *Bioinformatics* **27**: 1466-1472.

629 Dunn MF & Becerra-Rivera VA (2023) The biosynthesis and functions of polyamines in the
630 interaction of plant growth-promoting rhizobacteria with plants. *Plants* **12**: 2671.

631 Escudero JA, Loot C & Mazel D (2018) Integrons as adaptive devices. *Molecular mechanisms*
632 *of microbial evolution* 199-239.

633 Essakhi S, Cesbron S, Fischer-Le Saux M, Bonneau S, Jacques M-A & Manceau C (2015)
634 Phylogenetic and variable-number tandem-repeat analyses identify nonpathogenic
635 *Xanthomonas arboricola* lineages lacking the canonical type III secretion system. *Applied*
636 *and Environmental Microbiology* **81**: 5395-5410.

637 Galperin MY, Vera Alvarez R, Karamycheva S, Makarova KS, Wolf YI, Landsman D & Koonin
638 EV (2025) COG database update 2024. *Nucleic Acids Research* **53**: D356-D363.

639 Garita-Cambronero J, Palacio-Bielsa A, López MM & Cubero J (2017) Pan-genomic analysis
640 permits differentiation of virulent and non-virulent strains of *Xanthomonas arboricola* that
641 cohabit *Prunus* spp. and elucidate bacterial virulence factors. *Frontiers in microbiology* **8**:
642 573.

643 Getz LJ, Fairburn SR, Vivian Liu Y, Qian AL & Maxwell KL (2025) Integrons are anti-phage
644 defence libraries in *Vibrio parahaemolyticus*. *Nature Microbiology* 1-10.

645 Ghaly TM, Tetu SG & Gillings MR (2021) Predicting the taxonomic and environmental
646 sources of integron gene cassettes using structural and sequence homology of attC sites.
647 *Communications biology* **4**: 946.

648 Ghaly TM, Geoghegan JL, Alroy J & Gillings MR (2019) High diversity and rapid spatial
649 turnover of integron gene cassettes in soil. *Environmental Microbiology* **21**: 1567-1574.

650 Ghaly TM, Geoghegan JL, Tetu SG & Gillings MR (2020) The peril and promise of integrons:
651 beyond antibiotic resistance. *Trends in microbiology* **28**: 455-464.

652 Ghaly TM, Gillings MR, Rajabal V, Paulsen IT & Tetu SG (2024) Horizontal gene transfer in
653 plant microbiomes: integrons as hotspots for cross-species gene exchange. *Frontiers in*
654 *Microbiology* **15**: 1338026.

655 Ghaly TM, Rajabal V, Russel D, Colombi E & Tetu SG (2025) EcoFoldDB: Protein structure-
656 guided functional profiling of ecologically relevant microbial traits at the metagenome scale.
657 *bioRxiv* 2025.2004. 2002.646905.

658 Ghaly TM, Tetu SG, Penesyan A, Qi Q, Rajabal V & Gillings MR (2022) Discovery of integrons
659 in Archaea: Platforms for cross-domain gene transfer. *Science Advances* **8**: eabq6376.

660 Ghaly TM, Penesyan A, Pritchard A, Qi Q, Rajabal V, Tetu SG & Gillings MR (2022) Methods
661 for the targeted sequencing and analysis of integrons and their gene cassettes from complex
662 microbial communities. *Microbial genomics* **8**: 000788.

Ghaly TM, Rajabal V, Penesyan A, Coleman NV, Paulsen IT, Gillings MR & Tetu SG (2023) Functional enrichment of integrons: Facilitators of antimicrobial resistance and niche adaptation. *Iscience* **26**.

Gillings M, Boucher Y, Labbate M, Holmes A, Krishnan S, Holley M & Stokes H (2008) The evolution of class 1 integrons and the rise of antibiotic resistance. *Journal of bacteriology* **190**: 5095-5100.

Gillings MR (2014) Integrons: past, present, and future. *Microbiology and molecular biology reviews* **78**: 257-277.

Gillings MR, Holley MP, Stokes H & Holmes AJ (2005) Integrons in *Xanthomonas*: a source of species genome diversity. *Proceedings of the National Academy of Sciences* **102**: 4419-4424.

Guerin É, Cambray G, Sanchez-Alberola N, Campoy S, Erill I, Da Re S, Gonzalez-Zorn B, Barbé J, Ploy M-C & Mazel D (2009) The SOS response controls integron recombination. *Science* **324**: 1034-1034.

Hall RM & Collis CM (1995) Mobile gene cassettes and integrons: capture and spread of genes by site-specific recombination. *Molecular microbiology* **15**: 593-600.

Heinzinger M, Weissenow K, Sanchez JG, Henkel A, Mirdita M, Steinegger M & Rost B (2024) Bilingual language model for protein sequence and structure. *NAR Genomics and Bioinformatics* **6**: lqae150.

Hipólito A, García-Pastor L, Vergara E, Jové T & Escudero JA (2023) Profile and resistance levels of 136 integron resistance genes. *npj Antimicrobials and Resistance* **1**: 13.

Huerta-Cepas J, Szklarczyk D, Heller D, Hernández-Plaza A, Forslund SK, Cook H, Mende DR, Letunic I, Rattei T & Jensen LJ (2019) eggNOG 5.0: a hierarchical, functionally and phylogenetically annotated orthology resource based on 5090 organisms and 2502 viruses. *Nucleic acids research* **47**: D309-D314.

Jain C, Rodriguez-R LM, Phillippy AM, Konstantinidis KT & Aluru S (2018) High throughput ANI analysis of 90K prokaryotic genomes reveals clear species boundaries. *Nature communications* **9**: 5114.

Kawano M, Aravind á & Storz G (2007) An antisense RNA controls synthesis of an SOS-induced toxin evolved from an antitoxin. *Molecular microbiology* **64**: 738-754.

Kieffer N, Hipólito A, Ortiz-Miravalles L, Blanco P, Delobelle T, Vizuete P, Ojeda FM, Jové T, Jurenas D & García-Quintanilla M (2025) Mobile integrons encode phage defense systems. *Science* **388**: eads0915.

Klemm P, Stadler PF & Lechner M (2023) Proteinortho6: pseudo-reciprocal best alignment heuristic for graph-based detection of (co-) orthologs. *Frontiers in bioinformatics* **3**: 1322477.

698 Langmead B & Salzberg SL (2012) Fast gapped-read alignment with Bowtie 2. *Nature*
699 *methods* **9**: 357-359.

700 Lemoine F & Gascuel O (2021) Gotree/Goalign: toolkit and Go API to facilitate the
701 development of phylogenetic workflows. *NAR Genomics and Bioinformatics* **3**: lqab075.

702 Loeff L, Walter A, Rosalen GT & Jinek M (2025) DNA end sensing and cleavage by the Shedu
703 anti-phage defense system. *Cell* **188**: 721-733. e717.

704 Loot C, Millot GA, Richard E, Littner E, Vit C, Lemoine F, Néron B, Cury J, Darracq B & Niault T
705 (2024) Integron cassettes integrate into bacterial genomes via widespread non-classical attG
706 sites. *Nature Microbiology* **9**: 228-240.

707 Löytynoja A (2013) Phylogeny-aware alignment with PRANK. *Multiple sequence alignment*
708 *methods,*p.^pp. 155-170. Springer.

709 Mazel D (2006) Integrons: agents of bacterial evolution. *Nature Reviews Microbiology* **4**:
710 608-620.

711 Mazel D, Dychinco B, Webb VA & Davies J (1998) A distinctive class of integron in the *Vibrio*
712 *cholerae* genome. *Science* **280**: 605-608.

713 Michael CA & Labbate M (2010) Gene cassette transcription in a large integron-associated
714 array. *BMC genetics* **11**: 1-13.

715 Néron B, Littner E, Haudiquet M, Perrin A, Cury J & Rocha EP (2022) IntegronFinder 2.0:
716 identification and analysis of integrons across bacteria, with a focus on antibiotic resistance
717 in Klebsiella. *Microorganisms* **10**: 700.

718 Paradis E & Schliep K (2019) ape 5.0: an environment for modern phylogenetics and
719 evolutionary analyses in R. *Bioinformatics* **35**: 526-528.

720 Parks DH, Chuvochina M, Rinke C, Mussig AJ, Chaumeil P-A & Hugenholtz P (2022) GTDB: an
721 ongoing census of bacterial and archaeal diversity through a phylogenetically consistent,
722 rank normalized and complete genome-based taxonomy. *Nucleic acids research* **50**: D785-
723 D794.

724 Patané JS, Martins J, Rangel LT, Belasque J, Digiampietri LA, Facincani AP, Ferreira RM,
725 Jaciani FJ, Zhang Y & Varani AM (2019) Origin and diversification of *Xanthomonas citri* subsp.
726 *citri* pathotypes revealed by inclusive phylogenomic, dating, and biogeographic analyses.
727 *BMC genomics* **20**: 1-23.

728 Pena MM, Bhandari R, Bowers RM, Weis K, Newberry E, Wagner N, Pupko T, Jones JB,
729 Woyke T & Vinatzer BA (2024) Genetic and functional diversity help explain pathogenic,
730 weakly pathogenic, and commensal lifestyles in the genus *Xanthomonas*. *Genome Biology*
731 *and Evolution* **16**: evae074.

732 Pereira BM, Österlund T, Eriksson KM, Backhaus T, Axelson-Fisk M & Kristiansson E (2020) A
733 comprehensive survey of integron-associated genes present in metagenomes. *BMC*
734 *genomics* **21**: 1-14.

735 Post V & Hall RM (2009) Insertion sequences in the IS 1111 family that target the attC
736 recombination sites of integron-associated gene cassettes. *FEMS microbiology letters* **290**:
737 182-187.

738 Price MN, Dehal PS & Arkin AP (2010) FastTree 2–approximately maximum-likelihood trees
739 for large alignments. *PloS one* **5**: e9490.

740 Qi Q, Ghaly TM, Rajabal V, Russell DH, Gillings MR & Tetu SG (2024) Vegetable phylloplane
741 microbiomes harbour class 1 integrons in novel bacterial hosts and drive the spread of
742 chlorite resistance. *Science of the Total Environment* **954**: 176348.

743 Raga-Carbajal E, Espin G, Ayala M, Rodríguez-Salazar J & Pardo-López L (2022) Evaluation of
744 a bacterial group 1 LEA protein as an enzyme protectant from stress-induced inactivation.
745 *Applied Microbiology and Biotechnology* **106**: 5551-5562.

746 Rajabal V, Ghaly TM, Egidi E, Ke M, Penesyan A, Qi Q, Gillings MR & Tetu SG (2024) Exploring
747 the role of mobile genetic elements in shaping plant–bacterial interactions for sustainable
748 agriculture and ecosystem health. *Plants, People, Planet* **6**: 408-420.

749 Rao MJ, Zuo H & Xu Q (2021) Genomic insights into citrus domestication and its important
750 agronomic traits. *Plant Communications* **2**.

751 Rowe-Magnus DA & Mazel D (2001) Integrons: natural tools for bacterial genome evolution.
752 *Current opinion in microbiology* **4**: 565-569.

753 Rowe-Magnus DA, Guerout A-M, Biskri L, Bouige P & Mazel D (2003) Comparative analysis of
754 superintegrons: engineering extensive genetic diversity in the Vibrionaceae. *Genome*
755 *research* **13**: 428-442.

756 Sapkota S, Mergoum M & Liu Z (2020) The translucens group of *Xanthomonas translucens*:
757 complicated and important pathogens causing bacterial leaf streak on cereals. *Molecular*
758 *plant pathology* **21**: 291-302.

759 Schepler-Luu V, Sciallano C, Stiebner M, Ji C, Boulard G, Diallo A, Auguy F, Char SN, Arra Y &
760 Schenstnyi K (2023) Genome editing of an African elite rice variety confers resistance against
761 endemic and emerging *Xanthomonas oryzae* pv. *oryzae* strains. *Elife* **12**: e84864.

762 Schwengers O, Jelonek L, Dieckmann MA, Beyvers S, Blom J & Goesmann A (2021) Bakta:
763 rapid and standardized annotation of bacterial genomes via alignment-free sequence
764 identification. *Microbial genomics* **7**: 000685.

765 Shannon P, Markiel A, Ozier O, Baliga NS, Wang JT, Ramage D, Amin N, Schwikowski B &
766 Ideker T (2003) Cytoscape: a software environment for integrated models of biomolecular
767 interaction networks. *Genome research* **13**: 2498-2504.

768 Stokes Ht & Hall R (1989) A novel family of potentially mobile DNA elements encoding
769 site-specific gene-integration functions: integrons. *Molecular microbiology* **3**: 1669-1683.

770 Strugeon E, Tilloy V, Ploy M-C & Da Re S (2016) The stringent response promotes antibiotic
771 resistance dissemination by regulating integron integrase expression in biofilms. *MBio* **7**:
772 10.1128/mbio. 00868-00816.

773 Tansirichaiya S, Mullany P & Roberts AP (2019) Promoter activity of ORF-less gene cassettes
774 isolated from the oral metagenome. *Scientific Reports* **9**: 8388.

775 Tesson F, Hervé A, Mordret E, Touchon M, d'Humières C, Cury J & Bernheim A (2022)
776 Systematic and quantitative view of the antiviral arsenal of prokaryotes. *Nature*
777 *communications* **13**: 2561.

778 Tetu SG & Holmes AJ (2008) A family of insertion sequences that impacts integrons by
779 specific targeting of gene cassette recombination sites, the IS 1111-attC group. *Journal of*
780 *bacteriology* **190**: 4959-4970.

781 Teufel F, Almagro Armenteros JJ, Johansen AR, Gíslason MH, Pihl SI, Tsirigos KD, Winther O,
782 Brunak S, von Heijne G & Nielsen H (2022) SignalP 6.0 predicts all five types of signal
783 peptides using protein language models. *Nature biotechnology* **40**: 1023-1025.

784 Thompson MK, Nocedal I, Culviner PH, Zhang T, Gozzi KR & Laub MT (2022) *Escherichia coli*
785 SymE is a DNA-binding protein that can condense the nucleoid. *Molecular microbiology* **117**:
786 851-870.

787 Timilsina S, Potnis N, Newberry EA, Liyanapathiranage P, Iruegas-Bocardo F, White FF, Goss
788 EM & Jones JB (2020) *Xanthomonas* diversity, virulence and plant–pathogen interactions.
789 *Nature Reviews Microbiology* **18**: 415-427.

790 Triplett LR, Hamilton J, Buell C, Tisserat N, Verdier V, Zink F & Leach J (2011) Genomic
791 analysis of *Xanthomonas oryzae i*solates from rice grown in the United States reveals
792 substantial divergence from known X. oryzae pathovars. *Applied and Environmental*
793 *Microbiology* **77**: 3930-3937.

794 Van Kempen M, Kim SS, Tumescheit C, Mirdita M, Lee J, Gilchrist CL, Söding J & Steinegger
795 M (2024) Fast and accurate protein structure search with Foldseek. *Nature biotechnology*
796 **42**: 243-246.

797 Vauterin L, Yang P, Alvarez A, Takikawa Y, Roth DA, Vidaver AK, Stall RE, Kersters K & Swings
798 J (1996) Identification of non-pathogenic *Xanthomonas* strains associated with plants.
799 *Systematic and applied microbiology* **19**: 96-105.

800 Xu S, Dai Z, Guo P, Fu X, Liu S, Zhou L, Tang W, Feng T, Chen M & Zhan L (2021) ggtreeExtra:
801 compact visualization of richly annotated phylogenetic data. *Molecular biology and*
802 *evolution* **38**: 4039-4042.

Yu G, Smith DK, Zhu H, Guan Y & Lam TTY (2017) ggtree: an R package for visualization and annotation of phylogenetic trees with their covariates and other associated data. *Methods in Ecology and Evolution* **8**: 28-36.

Zhang Z, Todeschini TC, Wu Y, Kogay R, Naji A, Rodriguez JC, Mondi R, Kaganovich D, Taylor DW & Bravo JP (2023) Kiwa is a bacterial membrane-embedded defence supercomplex activated by phage-induced membrane changes. *bioRxiv* 2023.2002. 2026.530102.

FIGURE AND TABLE LEGENDS

Figure 1 – Distribution of integron platforms in *Xanthomonas* groups 1 and 2. The maximum likelihood phylogenetic tree is based on a concatenated alignment of 120 top-ranked marker proteins. The tree was rooted at the midpoint. Tips are labelled with species names assigned with Genome Taxonomy Database phylogeny. Integrons were classified as present if the isolates carried a functional integron, *intI* only or an *attC* array only. Scale bar indicates substitutions per site.

Figure 2 – Phylogeny of *intI*. Sequences of *intI* longer than 900 bp were aligned with PRANK, stripped of gaps and used to infer the tree with FastTree. *IntI* from *Vibrio* sp. SCSIO 43136 (locus tag: J4N39_08275) was used as an outgroup. The scale bar indicates substitutions per site. Only bootstrap values 0.80 are shown. Group 1 *Xanthomonas* are indicated on the side of the plot.

Figure 3 – Integrons in *X. campestris*. The phylogeny of *X. campestris* was built using Realphy, using GCA_000007145.1 as a reference genome. The tree was rooted with GCA_000972745 (*X. arboricola*) then the tip was removed from the tree. Tip labels show pathovars. The scale bar indicates substitutions per site. A) Indicates the presence of a complete integron or *attC* sites in the *ilvD* locus, B) indicates the presence of *intI*, C) indicates the presence of a CALINs (cluster of *attC* sites) not in the ilvD locus. D) indicates whether IntI is predicted to be functional (full length). E) indicates the number of *attC* sites (number of cassettes) in the genome. Panel F) represents the distribution of orthologous genes among all cassettes carried by the corresponding isolate inferred with Proteinortho. Orthologous genes are listed in decreasing order based on the number of strains within the species that carry them.

Figure 4 – Integrons in *X. cissicola*. The phylogeny of *X. cissicola* was built using Realphy, using GCA_000007165.1 as a reference genome. The tree was rooted with GCA_000009165.1 (*X. euvesicatoria*) then the tip was removed from the tree. Tip labels show pathovars, which were assigned from the literature search. The scale bar indicates substitutions per site. A) Indicates the presence of a complete integron or *attC* sites in the *ilvD* locus, B) indicates the presence of *intI*, C) indicates the presence of a CALINs (cluster of *attC* sites) not in the ilvD locus. D) indicates the number of *attC* sites (number of cassettes)

840 in the genome. Panel E) represents the distribution of orthologous genes among the all the
841 cassettes carried by the corresponding isolate inferred with Proteinortho. Orthologous
842 genes are given in decreasing order based on the number of strains within the species that
843 carry them.

844 **Figure 5 – Horizontal transfer of cassettes among *Xanthomonas* species.** Cytoscape
845 network illustrating transfer of cassettes between species. Nodes represent *Xanthomonas*
846 species, species containing more than 10 genomes in the dataset are coloured as in Figure 1
847 (tip labels). Line width between species is proportional to the number of cassettes moved
848 between species.

849 **Figure S1 – Phylogeny of *Xanthomonas intI*.** A maximum likelihood phylogenetic tree of all
850 *intI* in *Xanthomonas*. *IntI* from *Vibrio* sp. SCSIO 43136 (locus tag: J4N39_08275) was used as
851 an outgroup. The tree was inferred with FastTree and rooted with *Vibrio* sp. SCSIO 43136,
852 the scale bar indicates substitutions per site. * indicates the *intI*s are not integrated adjacent
853 to *ilvD*.

854 **Figure S2 – Phylogeny of *ilvD*.** The maximum-likelihood phylogenetic tree of all *ilvD* in
855 *Xanthomonas*. *ilvD* from *Vibrio* sp. SCSIO 43136 was used as an outgroup. The tree was
856 inferred with FastTree and rooted at midpoint, the scale bar indicates substitutions per site.

857 **Figure S3 – Integrons in *X. arboricola*.** The phylogeny of *X. arboricola* was built using
858 Realphy, using GCA_000972745.1 as a reference genome. The tree was rooted with
859 GCA_001908755.1 (*X. hortorum*) then the tip was removed from the tree. Tip labels show
860 pathovars, which were assigned via literature search. The red triangle indicates the probable
861 acquisition of the *intI* variant. The scale bar indicates substitutions per site. A) Indicates the
862 presence of a complete integron or *attC* sites in the *ilvD* locus, B) indicates the presence of
863 *intI*, C) indicates the presence of a CALINs (cluster of *attC* sites) not in the ilvD locus. D)
864 indicates whether IntI is predicted to be functional (full length). E) indicates the number of
865 *attC* sites (number of cassettes) in the genome. Panel F) represents the distribution of
866 orthologous genes among the all cassettes carried by the corresponding isolate inferred
867 with Proteinortho. Orthologous genes are given in decreasing order based on the number of
868 strains within the species that carry them.

869 **Figure S4 – Integrons in *X. translucens*.** The phylogeny of *X. translucens* was built using
870 Realphy, using GCA_001021935.1 as reference genome. The tree was rooted with
871 GCA_000007145.1 (*X. campestris*) then the tip removed from the tree. Tip labels show
872 pathovars, which were assigned via literature search. The scale bar indicates substitutions
873 per site. A) Indicates the presence of a complete integron or *attC* sites in the *ilvD* locus, B)
874 inidicates the presence of *intI*, C) indicate the presence of a CALINs (cluster of *attC* sites) not
875 in the ilvD locus. D) indicates whether IntI is predicted to be functional (full length). E)
876 indicates the number of *attC* sites (number of cassettes) in the genome. Panel F) represents
877 the distribution of orthologous genes among the all the cassettes carried by the
878 corresponding isolate interfered with Proteinortho. Orthologous genes are ordered in
879 decreasing order based on the number of strains within the species that carry them.

880 **Figure S5 – Integrons in *X. euvesicatoria*.** The phylogeny of *X. euvesicatoria* was built using
881 Realphy, using GCA_000009165.1 as reference genome. The tree was rooted with
882 GCA_002759095.2 (*X. phaseoli*) then the tip removed from the tree. The scale bar indicates
883 substitutions per site. A) Indicates the presence of a complete integron or *attC* sites in the
884 *ilvD* locus, B) inidicates the presence of *intI*, C) indicate the presence of a CALINs (cluster of
885 *attC* sites) not in the ilvD locus. D) indicates whether IntI is predicted to be functional (full
886 length). E) indicates the number of *attC* sites (number of cassettes) in the genome. Panel F)
887 represents the distribution of orthologous genes among the all the cassettes carried by the
888 corresponding isolate interfered with Proteinortho. Orthologous genes are ordered in
889 decreasing order based on the number of strains within the species that carry them.

890 **Figure S6 – Integrons in *X. oryzae*.** The phylogeny of *X. oryzae* was built using Realphy, using
891 GCA_000007385.1 as reference genome. The tree was rooted with GCA_002759095.2 (*X.*
892 *phaseoli*) then the tip removed from the tree. Tip labels show pathovars, which were
893 assigned via literature search. The scale bar indicates substitutions per site. A) Indicates the
894 presence of a complete integron or *attC* sites in the *ilvD* locus, B) inidicates the presence of
895 *intI*, C) indicate the presence of a CALINs (cluster of *attC* sites) not in the ilvD locus. D)
896 indicates whether IntI is predicted to be functional (full length). E) indicates the number of
897 *attC* sites (number of cassettes) in the genome. Panel F) represents the distribution of
898 orthologous genes among the all the cassettes carried by the corresponding isolate
899 interfered with Proteinortho. Orthologous genes are ordered in decreasing order based on
900 the number of strains within the species that carry them.

901 **Figure S7 – Integrons in *X. phaseoli*.** The phylogeny of *X. phaseoli* was built using Realphy,
902 using GCA_008639345.1 as reference genome. The tree was rooted with GCA_000009165.1
903 (*X. euvesicatoria*) then the tip removed from the tree. Tip labels show pathovars, which
904 were assigned via literature search. The scale bar indicates substitutions per site. A)
905 Indicates the presence of a complete integron or *attC* sites in the *ilvD* locus, B) inidicates the
906 presence of *intI*, C) indicate the presence of a CALINs (cluster of *attC* sites) not in the ilvD
907 locus. D) indicates whether IntI is predicted to be functional (full length). E) indicates the
908 number of *attC* sites (number of cassettes) in the genome. Panel F) represents the
909 distribution of orthologous genes among the all the cassettes carried by the corresponding
910 isolate interfered with Proteinortho. Orthologous genes are ordered in decreasing order
911 based on the number of strains within the species that carry them.

912 **Figure S8 – Integrons in *X. hortorum*.** The phylogeny of *X. hortorum* was built using Realphy,
913 using GCA_002285515.1 as reference genome. The tree was rooted with GCA_905367715.1
914 (*X. arboricola*) then the tip removed from the tree. Tip labels show pathovars, which were
915 assigned via literature search. The scale bar indicates substitutions per site. A) Indicates the
916 presence of a complete integron or *attC* sites in the *ilvD* locus, B) indicates the presence of
917 *intI*, C) indicate the presence of a CALINs (cluster of *attC* sites) not in the *ilvD* locus. D)
918 indicates whether IntI is predicted to be functional (full length). E) indicates the number of
919 *attC* sites (number of cassettes) in the genome. Panel F) represents the distribution of
920 orthologous genes among the all the cassettes carried by the corresponding isolate
921 interfered with Proteinortho. Orthologous genes are ordered in decreasing order based on
922 the number of strains within the species that carry them.

Figure S9 – Integron gene cassette counts in *Xanthomonas*. Boxplot of the number of *attC* sites per genome grouped by plant of isolation and by species (only species with more than 10 genomes are shown). Letters indicate statistically different groups (Dunn's test with Bonferroni adjustment, $p<0.001$).

Table S1 – Integrons and number of cassettes in the *Xanthomonas* genomes used in this study